

# PCCP

Accepted Manuscript



This is an *Accepted Manuscript*, which has been through the Royal Society of Chemistry peer review process and has been accepted for publication.

*Accepted Manuscripts* are published online shortly after acceptance, before technical editing, formatting and proof reading. Using this free service, authors can make their results available to the community, in citable form, before we publish the edited article. We will replace this *Accepted Manuscript* with the edited and formatted *Advance Article* as soon as it is available.

You can find more information about *Accepted Manuscripts* in the [Information for Authors](#).

Please note that technical editing may introduce minor changes to the text and/or graphics, which may alter content. The journal's standard [Terms & Conditions](#) and the [Ethical guidelines](#) still apply. In no event shall the Royal Society of Chemistry be held responsible for any errors or omissions in this *Accepted Manuscript* or any consequences arising from the use of any information it contains.



Cite this: DOI: 10.1039/xxxxxxxxxx

## The importance of current contributions to shielding constants in density-functional theory

Sarah Reimann,<sup>a\*</sup> Ulf Ekström,<sup>a‡</sup> Stella Stopkowicz,<sup>a</sup> Andrew M. Teale,<sup>a,b</sup> Alex Borgoo,<sup>a</sup> and Trygve Helgaker<sup>a¶</sup>

Received Date

Accepted Date

DOI: 10.1039/xxxxxxxxxx

www.rsc.org/journalname

The sources of error in the calculation of nuclear-magnetic-resonance shielding constants determined by density-functional theory are examined. Highly accurate Kohn–Sham wave functions are obtained from coupled-cluster electron density functions and used to define accurate—but current independent—density-functional shielding constants. These new reference values, in tandem with high-accuracy coupled-cluster shielding constants, provide a benchmark for the assessment of errors in common density-functional approximations. In particular the role of errors arising in the diamagnetic and paramagnetic terms is investigated, with particular emphasis on the role of current-dependence in the latter. For carbon and nitrogen the current correction is found to be, in some cases, larger than 10 ppm. This indicates that the absence of this correction in general purpose exchange-correlation functionals is one of the main sources of error in shielding calculations using density functional theory. It is shown that the current correction improves the shielding performance of many popular approximate DFT functionals.

### 1 Introduction

Nuclear-magnetic-resonance (NMR) shielding constants describe how an externally applied magnetic field is modified by the electrons surrounding the nuclei. The rich information contained in this response has made NMR spectroscopies a key tool in experimental chemistry. The prediction and interpretation of NMR spectra is therefore an important application area of quantum chemistry. Moreover, the sensitivity of this experimentally accessible shift represents a valuable test for the electronic-structure methodologies of quantum chemistry. In particular, for the applicability of Kohn–Sham density-functional theory (DFT), it is important to improve on the poor performance<sup>1,2</sup> of existing density-functional approximations (DFAs). From a DFT point of view, these calculations also represent an important theoretical challenge since the prediction of NMR shieldings relies on the induced electron current-density dependence of the exact exchange–correlation functional<sup>3</sup> or, alternatively, on its explicit dependence on the magnetic field.<sup>4</sup> The development of current-dependent DFAs remains an open problem.<sup>5</sup> In particular, it has been observed that the inclusion of a current dependence based

on the free-electron-gas model does not lead to improved NMR shieldings.<sup>6–9</sup>

For the purpose of analyzing approximate schemes for the calculation of NMR shielding constants it is fruitful to write the shielding tensor as consisting of three terms,

$$\sigma = \sigma^{\text{dia}} + \sigma_{\rho}^{\text{para}} + \sigma_{\mathbf{j}}^{\text{para}}. \quad (1)$$

The first term is the diamagnetic shielding (as defined in Section 2.1) which depends on the electron density  $\rho$  only. The second term is the current-independent part of the paramagnetic shielding (defined in Section 2.2), while the last term contains the current dependence. It has long been appreciated that, with the use of popular DFAs, the errors in  $\sigma^{\text{dia}}$  are small,<sup>10</sup> and most development has been focused on improving the description of the paramagnetic shielding.<sup>11–15</sup> Until recently it has been assumed that  $\sigma_{\mathbf{j}}^{\text{para}}$  can be neglected.<sup>6</sup> However, new theoretical and computational developments have allowed the importance of the current dependence of DFAs to be studied in isolation and it was found that these effects are not small compared with the total error of the best DFAs.<sup>1</sup> This observation constitutes an incentive to develop a current correction to the exchange–correlation functional of existing current-independent DFAs. Since the current corrections are expected to be relatively small it is important that errors in the underlying DFA are well balanced and minimized where possible. The aim of this paper is to quantify the magnitude of the current contribution, to analyze other sources of error (originating from the electron density in the diamagnetic shielding),

<sup>a</sup> Department of Chemistry, Centre for Theoretical and Computational Chemistry, University of Oslo, P.O. Box 1033, Blindern, Oslo N-0315, Norway

<sup>b</sup> School of Chemistry, University of Nottingham, University Park, Nottingham NG7 2RD, United Kingdom

\* sarah.reimann@kjemi.uio.no

‡ ulf.ekstrom@kjemi.uio.no

¶ t.u.helgaker@kjemi.uio.no

48 and to suggest suitable DFAs to which further current corrections  
49 can be reliably applied.

50 We here study a collection of DFAs chosen to cover the fa-  
51 miliar sequence consisting of the local-density approximation  
52 (LDA<sup>16</sup>), generalized-gradient approximation (GGA) functionals  
53 (BLYP<sup>17,18</sup> and PBE<sup>19</sup>), hybrid functionals (B97<sup>20</sup> and B3LYP<sup>21</sup>),  
54 and meta-GGA functionals (TPSS<sup>22</sup>). We also include the KT2  
55 functional,<sup>14</sup> developed specifically for NMR shielding constants.  
56 Since a comparison with experiment requires a treatment of vi-  
57 brational effects,<sup>1</sup> we compare instead with accurate theoretical  
58 shielding constants calculated at a fixed molecular geometry us-  
59 ing coupled-cluster theory with single, double and perturbative  
60 triple excitations (CCSD(T)).<sup>23</sup>

61 The diamagnetic contribution to the shielding constant can  
62 be defined to depend only on the ground-state electron density.  
63 Therefore, we examine the error in the density calculated using  
64 different DFAs by comparison with the CCSD(T) reference density.  
65 In the absence of a field the exact exchange–correlation functional  
66 is purely density dependent. For such a purely density-dependent  
67 functional, which neglects current dependence but yields the ex-  
68 act charge density at zero field, the paramagnetic response is de-  
69 termined purely by the values of the orbitals and eigenvalues of  
70 the Kohn–Sham system. Using this fact we are able to calculate  
71 the  $\sigma_p^{\text{para}}$  term in Eq. (1) and distinguish errors originating from  
72 the neglect of current dependence from those coming from the  
73 use of an approximate exchange–correlation functional.

## 74 2 Theory

### 75 2.1 NMR shielding constants

76 The NMR shielding tensor  $\sigma_K$  associated with nucleus  $K$  is de-  
77 fined as the second-order derivative of the molecular electronic  
78 energy with respect to the external magnetic field with flux den-  
79 sity  $\mathbf{B}$  and the magnetic moment  $\mathbf{M}_K$  of that nucleus at  $\mathbf{B} = 0$  and  
80  $\mathbf{M}_K = 0$ ,<sup>24</sup>

$$81 \quad \sigma_K = \left. \frac{d^2 E}{d\mathbf{B} d\mathbf{M}_K} \right|_{\mathbf{B}, \mathbf{M}_K = 0}. \quad (2)$$

82 In common with all second-order magnetic properties, the shield-  
83 ing tensor can be decomposed into diamagnetic and paramag-  
84 netic parts,

$$85 \quad \sigma_K = \sigma_K^{\text{dia}} + \sigma_K^{\text{para}}, \quad (3)$$

86 but this decomposition is not unique. Throughout this work  
87 we use London atomic orbitals<sup>25</sup> to ensure gauge origin inde-  
88 pendence of our results. We follow the convention that the  
89 diamagnetic part depends only on the ground-state density; all  
90 terms describing some form of response to the field, including  
91 the response encoded in the London atomic orbitals or gauge-  
92 invariant atomic orbitals (GIAOs), are contained in the paramag-  
93 netic part.<sup>26</sup> Specifically, we define the diamagnetic part as (omit-  
94 ting here and elsewhere the summation over electrons)

$$95 \quad \sigma_K^{\text{dia}} = \frac{1}{2} \left\langle 0 \left| \frac{\mathbf{r}_0^T \mathbf{r}_K - \mathbf{r}_0 \mathbf{r}_K^T}{r_K^3} \right| 0 \right\rangle, \quad (4)$$

96 where  $\mathbf{r}_K = \mathbf{r} - \mathbf{R}_K$  is the position vector of the electron relative  
97 that of the nucleus  $\mathbf{R}_K$ , and  $\mathbf{r}_0 = \mathbf{r} - \mathbf{R}_0$  is the position vector

98 of the electron relative to the gauge origin  $\mathbf{R}_0$ . Unless other-  
99 wise stated, atomic units are used in this paper. Setting the  
100 gauge origin at nucleus  $K$ , the diamagnetic NMR shielding con-  
101 stant becomes directly proportional to the expectation value of  
102 the Coulomb interaction at the nucleus

$$103 \quad \sigma_K^{\text{dia}} = \frac{1}{3} \text{Tr} \sigma_K^{\text{dia}} = \frac{1}{3} \left\langle 0 \left| \frac{1}{r_K} \right| 0 \right\rangle. \quad (5)$$

104 In the present paper, the quality of the total shielding constant  $\sigma_K$   
105 and its diamagnetic part  $\sigma_K^{\text{dia}}$  calculated with different DFAs will  
106 be assessed by a direct comparison with accurate CCSD(T) values,  
107 thereby quantifying also the error in the paramagnetic part  $\sigma_K^{\text{para}}$ .  
108 We also analyze the sources of error in  $\sigma_K^{\text{para}}$  and, in particular,  
109 quantify the error incurred by neglecting the field dependence of  
110 the exchange–correlation functional, as discussed in the following  
111 subsection.

### 112 2.2 Magnetic perturbations in current-independent DFT

113 Here we are concerned only with pure density functionals, i.e.  
114 LDA, GGA, and the exact universal functional. When the cur-  
115 rent dependence of the exchange–correlation energy is neglected,  
116 the ground-state energy can be decomposed into familiar com-  
117 ponents: the non-interacting kinetic energy  $T_s(\rho, \mathbf{A})$  with a de-  
118 pendence on the vector potential  $\mathbf{A}$ , the exchange–correlation–  
119 Hartree energy  $E_{\text{xch}}(\rho)$ , and the interaction between the elec-  
120 trons and the external scalar potential  $v$  set up by the nuclei,  
121 ( $v, \rho$ ):

$$122 \quad E(v, \mathbf{A}) = \inf_{\rho} \{ T_s(\rho, \mathbf{A}) + E_{\text{xch}}(\rho) + (\rho, v) \mid \int \rho(\mathbf{r}) d\mathbf{r} = N \}. \quad (6)$$

123 Note that within this approximation,  $E_{\text{xch}}$  here remains the stan-  
124 dard “non-magnetic” exchange–correlation–Hartree energy.

125 We now show that, for a current independent functional of  
126 the above form, the second derivative with respect to the vector  
127 potential is simply the second derivative of the non-interacting  
128 kinetic energy. Assuming the existence of a minimizing density  
129  $\rho_{\text{GS}}(v, \mathbf{A})$  and that the derivatives are well defined (for a discus-  
130 sion of this point in conventional DFT see Ref. 27), the DFT Euler  
131 equation is given by

$$132 \quad \frac{\delta}{\delta \rho(\mathbf{r})} (T_s(\rho, \mathbf{A}) + E_{\text{xch}}(\rho)) + v(\mathbf{r}) = \mu. \quad (7)$$

For closed-shell systems (which are considered here), the first  
derivative of  $T_s$  with respect to  $\mathbf{A}$  vanishes since  $T_s(\rho, \mathbf{A})$  is an  
even function of  $\mathbf{A}$  at  $\mathbf{A} = \mathbf{0}$ . The Euler equation is therefore au-  
tomatically satisfied to first order in  $\mathbf{A}$ , implying that the density  
depends on  $\mathbf{A}$  only to second order. Setting  $\rho = \rho_0 + \rho_2 \mathbf{A}^2$  and ex-

panding the ground-state energy to second order in  $\mathbf{A}$ , we obtain

$$\begin{aligned}
 E(v, \mathbf{A}) = & T_s(\rho_0, 0) + E_{\text{xCH}}(\rho_0) + (\rho_0, v) \\
 & + \frac{1}{2} \iint \frac{\delta^2 T_s(\rho, \mathbf{A})}{\delta \mathbf{A}(\mathbf{r}) \delta \mathbf{A}(\mathbf{r}')} \Big|_{(\rho_0, 0)} \mathbf{A}(\mathbf{r}) \mathbf{A}(\mathbf{r}') \text{d}\mathbf{r} \text{d}\mathbf{r}' \\
 & + \int \left( \frac{\delta (T_s(\rho, \mathbf{A}) + E_{\text{xCH}}(\rho))}{\delta \rho(\mathbf{r})} \Big|_{(\rho_0, 0)} \right. \\
 & \left. + v(\mathbf{r}) \right) \rho_2(\mathbf{r}) \mathbf{A}(\mathbf{r})^2 \text{d}\mathbf{r}, \quad (8)
 \end{aligned}$$

where the last term vanishes because the Euler equation is satisfied for the reference state; since the density variations are particle-number preserving for all  $\mathbf{A}$ , the integral  $\int \rho_2(\mathbf{r}) \mathbf{A}^2(\mathbf{r}) \text{d}\mathbf{r}$  vanishes. Hence, the second derivative of a closed-shell ground-state energy with respect to the vector potential, at zero vector potential, is simply the second derivative of the non-interacting kinetic energy. Note that the exchange–correlation kernel contributions, arising from the second derivative of  $E_{\text{HXC}}$ , appear only at higher orders in  $\mathbf{A}$ . This well-known result is usually stated for LDA and GGA functionals in terms of the “magnetic Hessian”.<sup>28</sup> The present proof relies only on the observation that  $T_s$  is even in  $\mathbf{A}$  at  $\mathbf{A} = \mathbf{0}$ .

For the shielding tensor, we then insert  $\mathbf{A} = \mathbf{A}_0 + \mathbf{A}_K$ , where  $\mathbf{A}_0$  and  $\mathbf{A}_K$  are the vector potentials associated with  $\mathbf{B}$  and  $\mathbf{M}_K$ , respectively, to obtain the usual formula in terms of Kohn–Sham orbitals and eigenvalues. Neglecting the contribution due to London orbitals the expression is<sup>6</sup>

$$\sigma_{\rho}^{\text{para}} = - \sum_i^{\text{occ}} \sum_a^{\text{virt}} \frac{\langle i | \mathbf{l} | a \rangle \langle a | \mathbf{l}_K^T r_K^{-3} | i \rangle + \text{h.c.}}{\epsilon_a - \epsilon_i}, \quad (9)$$

where h.c. is the hermitian conjugate and  $\mathbf{l}$  is the angular momentum operator.

It should be noted that by employing Eq. (8) the shielding tensor (or indeed other magnetic properties) can be computed for an arbitrary input density without knowledge of the exact exchange–correlation (XC) functional. All that is required are the second derivatives of  $T_s$ , which can be obtained from the Kohn–Sham wave function corresponding to  $\rho$ . This wave function can be obtained by various approaches, for example the Zhao–Morrison–Parr<sup>29</sup> method employed by Wilson and Tozer<sup>13</sup> for the calculation of shieldings. We instead use the method outlined in Section 3.

### 3 Computational Details

We have evaluated total and diamagnetic NMR shielding constants for a set of small atoms and molecules, at the CCSD(T) equilibrium geometries. In the next section, we compare wavefunction quantities from Hartree–Fock (HF) theory, second-order Møller–Plesset (MP2) perturbation theory, and CCSD(T) theory with those from a representative set of standard DFAs. To quantify the error arising from the neglect of the current dependence in the DFA, we also present Kohn–Sham shielding constants obtained from accurate CCSD(T) densities using an established in-

version scheme.<sup>30,31</sup>

The coupled-cluster calculations of shielding constants were performed using CFOUR.<sup>32</sup> A development version of DALTON<sup>33,34</sup> was used for all other calculations, except those involving the TPSS functional. The latter were evaluated with the LONDON quantum-chemistry software.<sup>8,35,36</sup>

Meta-GGAs, such as TPSS, depend on the Kohn–Sham kinetic energy density  $\tau_0(\mathbf{r}) = \frac{1}{2} \sum_i^{\text{occ}} \|\nabla \phi_i(\mathbf{r})\|^2$ . In magnetic fields this quantity must be generalized in a gauge-invariant fashion. Maximoff and Scuseria<sup>37</sup> suggested the use of the physical kinetic energy density

$$\tau_{\text{MS}} = \tau_0 + \mathbf{j}_p \cdot \mathbf{A} + \frac{1}{2} \rho \mathbf{A}^2. \quad (10)$$

This quantity is gauge invariant but introduces an explicit dependence of the XC energy on the vector potential  $\mathbf{A}$ . Another problem is that the so-called “isoorbital indicator” used in the TPSS functional can take unphysical values in magnetic fields.<sup>38</sup> We denote the TPSS functional with this choice of  $\tau$  by cTPSS( $\tau_{\text{MS}}$ ). Another option is to use the gauge-invariant kinetic energy proposed by Dobson,<sup>39</sup> and used by Becke<sup>40</sup> and Tao,<sup>41</sup>

$$\tau_{\text{D}} = \tau_0 - \frac{\mathbf{j}_p^2}{2\rho}. \quad (11)$$

This kinetic energy density depends only on the paramagnetic current, and not on the external magnetic field. It also leads to physical isoorbital indicator values. This functional, here denoted cTPSS( $\tau_{\text{D}}$ ), is equivalent to that introduced by Bates and Furché for the calculation of excitation energies in Ref.<sup>42</sup> and its implementation and application to magnetic properties will be discussed in detail elsewhere.<sup>43</sup> For reference we also compute shielding values using the gauge dependent  $\tau_0$ , with the gauge origin placed on the molecular center of mass. We refer to this functional as TPSS( $\tau_0$ ). The shielding constants with the TPSS and cTPSS functionals presented in this work were obtained by a numerical differentiation, using finite magnetic fields – for further details see Ref.<sup>8</sup>.

We used the augmented correlation-consistent basis sets by Dunning and coworkers, known to be suitable for the computation of magnetic properties.<sup>44</sup> We investigated basis-set convergence and found the aug-cc-pVQZ basis<sup>45,46</sup> to be appropriate for the systems studied in this work. Cartesian Gaussian basis sets have been used throughout all calculations.

To ensure gauge-origin independence of the total shieldings, we employ London orbitals.<sup>25,47</sup> We note that the DALTON program uses a definition for the diamagnetic part of the NMR shielding constant that includes a contribution from the London atomic orbitals. We here use the definition in Eq. (4), where we obtain the corresponding values using separate calculations without London orbitals.

In order to isolate the effect of the current dependent exchange–correlation energy on the shieldings we calculate the non-interacting Kohn–Sham potential, orbitals and orbital energies corresponding to a specific electron density using the procedure of Wu and Yang.<sup>30</sup> The paramagnetic shielding constants are then obtained using Eq. (9). These calculations were carried out using a locally modified version of the DALTON program.<sup>31</sup> Total shield-

ing constants calculated using this method will be called  $\sigma_{\text{KS}}$  in the following.

## 4 Results and discussion

In this section, we analyze the errors coming from the diamagnetic and the paramagnetic parts of the NMR shieldings to gain insight into the limitations of common DFAs and the role of current dependence. We study a set of small systems (He, Ne, HF, CO, N<sub>2</sub>, H<sub>2</sub>O, NH<sub>3</sub>, and CH<sub>4</sub>) for which we computed accurate CCSD(T) reference values, and also obtained the corresponding accurate Kohn–Sham non-interacting wave functions.

### 4.1 Current-dependence of DFT shielding constants

We begin by assessing the importance of  $\sigma_j^{\text{para}}$  relative to the diamagnetic and current-independent contributions to the shielding constant in Eq. (1) for the molecules in the test set, see Table 1. In this table,  $\sigma$  is the total shielding constant calculated at the CCSD(T) level of theory, and the diamagnetic part  $\sigma^{\text{dia}}$  is the expectation value in Eq. (4) calculated from the CCSD(T) density matrix. To obtain the paramagnetic density and current contributions, we have first calculated the total current free shielding constant  $\sigma_{\text{KS}}$  using the Wu–Yang scheme with the CCSD(T) density as described in Section 3 and then used the relations  $\sigma_{\rho}^{\text{para}} = \sigma_{\text{KS}} - \sigma^{\text{dia}}$  and  $\sigma_j^{\text{para}} = \sigma - \sigma_{\text{KS}}$ .

From Table 1, we first note that the current contribution is typically one to two orders of magnitude smaller than the diamagnetic and paramagnetic contributions to the shielding constants. However, since the diamagnetic and paramagnetic contributions are always of opposite sign and may nearly cancel, the current contribution to the shielding cannot always be neglected and sometimes becomes important. For example, in  $\sigma_{\text{C}}$  in CO, the total shielding is 5.4 ppm with a current contribution of 11.0 ppm, twice as large as the total shielding; in this particular case, the total diamagnetic and paramagnetic contributions are 327.0 and  $-332.6$  ppm. In N<sub>2</sub>, the situation is similar but less dramatic, the total shielding constant being  $-57.4$  ppm with a large current contribution of 13.3 ppm. Clearly, the current contribution to the shielding constants cannot in general be neglected, at least for non-hydrogen: for the non-hydrogen atoms in Table 1, the current contribution ranges from 1.7 to 13.3 ppm. For proton shieldings, the current contribution is negligible, contributing in all cases less than 1% to the total shielding constant. Although our estimated error, due to approximation in the Wu–Yang procedure, on the current contribution lies below 0.05 ppm for the H atom, we cannot be completely confident that the negative sign of the current contribution for this atom is not a basis set error. For the other atoms the current contribution is clearly positive.

The main source of error in the calculated  $\sigma_j^{\text{para}}$  values arise from the orbital and potential basis sets, as well as optimization thresholds, employed in the Wu–Yang calculations. By studying the convergence of the results in terms of the potential and orbital basis sets (we use the same family of aug-cc-pVXZ sets for both) when going between the QZ and 5Z sets we can estimate the errors in Table 1, which are listed in the last column of the same table. The by far largest error, most likely smaller than 1.5 ppm,

is in the current contribution for N<sub>2</sub>, but this and other errors do not change any conclusion or has any significant impact on the statistic in the following sections.

Finally, we note that the current contribution is positive for all heavy atoms in Table 1, increasing the shielding constant and reducing the overall paramagnetic contribution. For the protons, by contrast, the current contribution is negative in all cases. We cannot rule out that the very small negative current contribution for proton is a numerical artifact; however, this seems unlikely in view of the high degree of convergence for the proton shielding of the HF molecule. It appears, therefore, that the current contribution to shielding constants can be both negative and positive.

### 4.2 Diamagnetic shielding constants and the role of the electron density

Since the current contribution to the shieldings in the previous subsection was shown to sometimes be as large as 10 ppm it would be a worthwhile effort to develop an approximate DFT expression for this correction. For this reason it is important to investigate the sources of errors in the diamagnetic and paramagnetic contributions for existing DFAs. For an evaluation of the diamagnetic shielding constants, we compare calculated DFA, HF, and MP2 diamagnetic contributions to the shielding constants with the corresponding CCSD(T) values. In Table 2, we report the mean and standard deviation of the error in  $\sigma^{\text{dia}}$  for the different models. Although only a limited number of systems are considered the methods can be qualitatively ranked, in order from smallest to largest absolute errors, as CCSD, MP2 < PBE, B3LYP, B97, BLYP, TPSS, HF < LDA < KT2. Note that both forms of cTPSS give the same result as TPSS, since the diamagnetic shielding is defined as not including any current effects. The most remarkable observation is that the KT2 functional, which has been optimized for improving total NMR shielding constants, gives an error in the diamagnetic shielding at least an order of magnitude larger than all other methods. We note that the hybrid functionals B3LYP and B97 and the meta-GGA functional TPSS are not significantly better than the best GGA functionals, but most DFAs are clearly outperformed by MP2 theory. The exception is PBE, which gives very high quality diamagnetic shieldings for our test set.

Although the diamagnetic part of the shielding constant is the focus of this section, it is just one measure of a “good density”. Exchange–correlation functionals are typically optimized for ground-state energies, which include the expectation value  $\langle r^{-1} \rangle$ . We therefore expect these functionals to give good diamagnetic shieldings, but it is nevertheless worthwhile to investigate the density error in more detail. In the paramagnetic part of the shielding [Eq. (9)] the presence of the  $r^{-3}$  operator is expected to give larger weights to density errors near the nucleus, compared to the diamagnetic term.

We therefore investigate the electron density errors of the different methods in a more general sense. In Figure 2 the density errors  $\Delta\rho(r)$ ,  $r\Delta\rho(r)$ ,  $r^2\Delta\rho(r)$  and  $r^4\Delta\rho(r)$  are plotted as functions of  $r$  (where  $\Delta\rho = \rho - \rho_{\text{CCSD(T)}}$ ) for the helium and neon atoms. The first of these shows the local density error at different locations in the atom, and integrates to the expectation value  $\langle r^{-2} \rangle$ .

**Table 1** The diamagnetic, current independent paramagnetic and current dependent paramagnetic parts of the benchmark shielding constants in ppm, calculated at the CCSD(T) level, together with estimates of the absolute error due to the Wu-Yang procedure.

Molecule	$\sigma$	=	$\sigma^{\text{dia}}$	+	$\sigma_p^{\text{para}}$	+	$\sigma_j^{\text{para}}$	Err
He	59.9		59.9		0		0	0
Ne	552.0		552.0		0		0	0
HF(H)	28.9		108.6		-79.5		-0.2	0.05
CH <sub>4</sub> (H)	31.3		87.7		-56.3		-0.1	0.05
NH <sub>3</sub> (H)	31.5		95.5		-63.9		-0.1	0.05
H <sub>2</sub> O(H)	30.8		102.4		-71.4		-0.2	0.05
CH <sub>4</sub> (C)	199.4		297.0		-104.9		7.3	0.05
CO(C)	5.4		327.0		-332.6		11.0	0.05
NH <sub>3</sub> (N)	270.7		354.5		-89.4		5.6	0.5
N <sub>2</sub> (N)	-57.4		384.7		-455.4		13.3	1.5
H <sub>2</sub> O(O)	337.8		416.2		-82.0		3.6	0.2
CO(O)	-51.7		444.8		-501.0		4.5	0.5
HF(F)	420.8		482.1		-63.0		1.7	0.5

**Table 2** Mean absolute density error  $I$  (Eq. 12), mean and standard deviation (S) of the shielding error (in ppm)  $\Delta\sigma^{\text{dia}} = \sigma^{\text{dia}} - \sigma_{\text{CCSD(T)}}^{\text{dia}}$  (left),  $\Delta\sigma = \sigma - \sigma_{\text{CCSD(T)}}$  (middle) and  $\Delta\sigma_{\text{KS}} = \sigma - \sigma_{\text{KS}}$  (right). Here  $\sigma_{\text{KS}}$  is the current independent DFT shielding computed from the CCSD(T) densities. This method is also labeled KS(CCSD(T)) in the table. The  $I$  value for TPSS and cTPSS was omitted for technical reasons.

Method	$I$	$\Delta\sigma^{\text{dia}}$	$S(\Delta\sigma^{\text{dia}})$	$\Delta\sigma$	$S(\Delta\sigma)$	$\Delta\sigma_{\text{KS}}$	$S(\Delta\sigma_{\text{KS}})$
LDA	0.14	-1.01	0.53	-9.60	14.61	-6.02	11.50
BLYP	0.13	0.19	0.15	-9.62	11.36	-6.04	7.71
PBE	0.08	0.03	0.11	-8.58	10.91	-5.00	7.61
KT2	0.13	2.51	1.66	-2.00	4.14	1.58	5.16
B97	0.05	0.15	0.05	-9.18	11.79	-5.60	8.39
B3LYP	0.07	0.11	0.09	-10.36	13.32	-6.78	9.65
TPSS( $\tau_0$ )	-	0.22	0.09	-4.44	4.68	-0.86	2.95
cTPSS( $\tau_D$ )	-	0.22	0.09	-7.15	8.29	-3.57	4.92
cTPSS( $\tau_{\text{MS}}$ )	-	0.22	0.09	-6.57	7.20	-2.99	3.87
HF	0.14	-0.15	0.34	-11.59	17.85		
MP2	0.03	-0.01	0.09	3.80	5.10		
CCSD	0.02	0.01	0.04	-1.28	2.03		
KS(CCSD(T))	0	0	0	-3.57	4.59		

333 The second quantity integrates to the error in the expectation  
334 value  $\langle r^{-1} \rangle$ , while the third integrates to the error in the num-  
335 ber of electrons (which is zero), and the fourth integrates to the  
336 error in the atomic quadrupole moment.

337 Considering the maximum error at different  $r$  in the two first  
338 rows of Figure 2, rather than the average error appearing in the  
339 diamagnetic shielding integral, we obtain a ranking CCSD < MP2  
340 < TPSS, HF < PBE, B3LYP, B97, BLYP < KT2 < LDA. The CCSD  
341 error is not plotted, to reduce visual clutter, but this error is in  
342 all cases smaller than that of all other methods. For simplicity  
343 the GGA functionals are not distinguishable in the figure, but the  
344 overall trends and spread are clearly visible. In particular, the  
345 density error near the nucleus is very large for all DFAs. However,  
346 this error is cancelled by opposite errors further away from the  
347 nucleus, leading overall to good accuracy of the  $\langle r^{-1} \rangle$  expectation  
348 value relevant for the diamagnetic shielding.

349 From the different weightings shown in Figure 2, we conclude  
350 that a similar trend holds for the quadrupole moments. How-  
351 ever, the advantage of HF is now less pronounced and the KT2 er-  
352 ror less severe. The TPSS functional loses its advantage over the  
353 other DFAs in the regions far away from the nucleus, but these are  
354 less relevant for shieldings. We note that a radial density analysis  
355 has recently been utilized to understand density errors associated  
356 with the correlation treatment in DFAs in Refs. 48,49. Our density  
357 study differs slightly in the choices of functionals, and importantly  
358 includes data for the TPSS meta-GGA functional. This functional  
359 is found to be the best performing DFA in our benchmark. While  
360 it has the same error trends (i.e. too large density at the nucleus  
361 and similar density error oscillations away from the nucleus) as  
362 the GGA functionals it has the smallest absolute errors and more  
363 mild oscillations. Since the HF density errors often are of oppo-  
364 site sign to the DFA errors one might think that hybrid functionals  
365 would be good overall performers. This is not the case for the  
366 B3LYP functional, which gives results in line with the pure GGA  
367 functionals.

368 Figure 1 shows the error  $\Delta\rho$  along the bond axis for the N<sub>2</sub>  
369 and H<sub>2</sub>O molecules. In both cases, it is clear that there exist re-  
370 gions near the nuclei, up to the inner-valence region, where the  
371 Kohn-Sham calculations yield densities considerably worse than  
372 HF. However, as can be seen from the mean of the integral of the  
373 absolute density errors,

$$374 \quad I = \int |\rho(\mathbf{r}) - \rho_{\text{CCSD(T)}}(\mathbf{r})| d\mathbf{r}, \quad (12)$$

375 presented in Table 2, the global density error is somewhat smaller  
376 for the approximate Kohn-Sham calculations. BLYP has a similar  
377 absolute error  $I$  as HF, but since the errors at a particular point  
378 in space often have opposite sign (see Fig. 2) it is not surprising  
379 that the hybrid functional B3LYP reduces the value of  $I$  signifi-  
380 cantly. However, the pure GGA functionals PBE and B97 both  
381 perform similar to, or better than, B3LYP by the same measure.  
382 However, the value of  $I$  seems to be only weakly correlated with  
383 the quality of the diamagnetic shielding. The KT2 functional has  
384 a large diamagnetic error but the value of  $I$  is not larger than for  
385 BLYP. This emphasizes the physical fact that it is the density near  
386 each atomic nucleus which is important for the shielding of that

387 particular nucleus.

388 The reason that the DFAs perform better than the HF method  
389 according to these measures is that the errors, while large, are lo-  
390 calized to small regions near the nuclei. Furthermore, the density  
391 errors oscillate about zero as we move away from the nucleus,  
392 as seen in Figure 1. Around the nuclei all DFA densities show  
393 a much larger error than the HF method; however, as we move  
394 away from the nuclei, the DFA densities improve relative to the  
395 HF density. It should also be pointed out that the absolute value  
396 of the DFA error is about two orders of magnitude larger in the  
397 core region than in the valence region. In other words, the HF  
398 density has, relative to the CCSD(T) density, a more uniform er-  
399 ror, whereas the DFAs perform better in the valence region but  
400 are much worse in the core region.

401 To summarize this section we note that for the worst perform-  
402 ing functionals for the diamagnetic shieldings (LDA and KT2) the  
403 plot of the density errors clearly show the origin of their poor  
404 diamagnetic performance. However, investigating the PBE densi-  
405 ties, which give the best diamagnetic shieldings of all the tested  
406 DFAs, reveals that this good performance is a result of error can-  
407 cellation. The TPSS functional, on the other hand, has smaller  
408 maximum errors and its gauge-independent cTPSS variants may  
409 be a more promising functional for shieldings, considering the  
410 (here unquantified) effect of the core density on the paramag-  
411 netic shielding tensor.

412 Finally we note that, for the considered molecules, MP2 gives  
413 densities that are of much higher quality than all considered DFAs,  
414 but as can be seen in Table 2 such high quality densities are  
415 not needed for high (i.e. sub-ppm) accuracy in the diamagnetic  
416 shielding constants. The error in total MP2 shieldings is thus at-  
417 tributed to the incomplete treatment of electron correlation in  
418  $\sigma^{\text{para}}$  by the MP2 method.

#### 419 4.3 Total NMR shielding constants

420 Table 2 contains the mean and standard deviation of the error in  
421 the NMR shielding constant for the different methods. We first  
422 consider the error with respect to the CCSD(T) shieldings ( $\Delta\sigma$  in  
423 columns five and six), which include current contributions. One  
424 should note that the CO and N<sub>2</sub> molecules are the most difficult  
425 cases for all the methods. This means that the average error  
426 is strongly influenced by these two molecules, emphasizing the  
427 molecules with the largest errors.

428 Regarding the error in the total shielding, we obtain a ranking  
429 CCSD < KT2, MP2 < TPSS( $\tau_0$ ), cTPSS( $\tau_{\text{MS}}$ ), cTPSS( $\tau_{\text{D}}$ ) < PBE,  
430 B97, BLYP < B3LYP, LDA < HF. The KT2 exchange–correlation  
431 functional clearly benefits from having been constructed by fitting  
432 to experimental shielding data, performing well for total shielding  
433 constants in spite of its poor performance for the diamagnetic  
434 part. The KT2 errors have roughly equal contributions from the  
435 diamagnetic and paramagnetic parts, whereas the error in the  
436 paramagnetic term dominates for all other DFAs, among which  
437 TPSS( $\tau_0$ ) is a clear winner.

438 Surprisingly, the current including, gauge-independent variants  
439 of cTPSS both perform slightly worse than TPSS( $\tau_0$ ), although  
440 they still give better values than the remaining DFAs. Since  $\tau_0$  de-

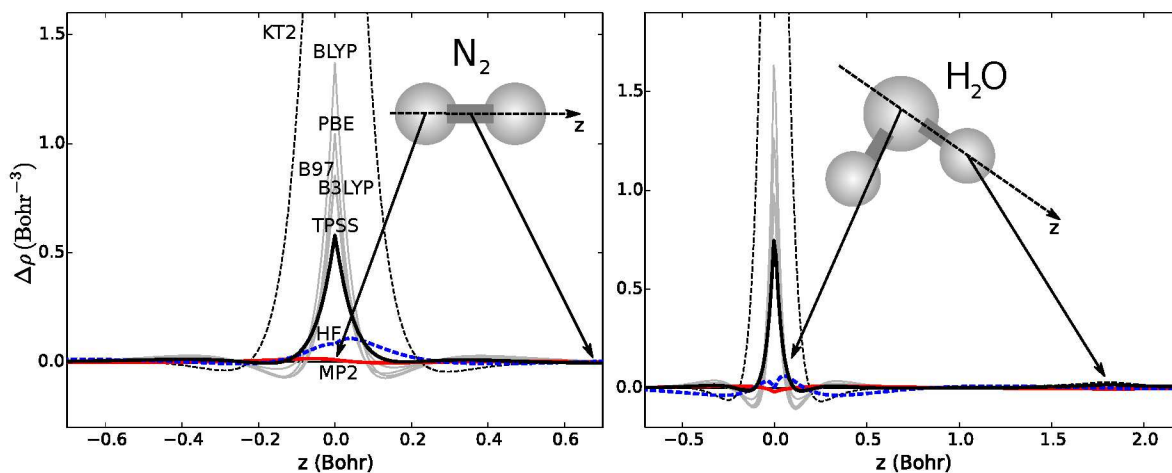


**Fig. 1** The density error  $\Delta\rho = \rho - \rho_{\text{CCSD(T)}}$  for  $\text{N}_2$  and  $\text{H}_2\text{O}$  is plotted along the molecular axis and O-H bond respectively. Line types are the same as in Fig. 2

441 depends on the choice of gauge the TPSS( $\tau_0$ ) functional cannot be  
 442 recommended for general use, but the results seem relatively in-  
 443 sensitive to small shifts in gauge origin. Moving the gauge origin  
 444 from the center of mass to the shielding nucleus in  $\text{N}_2$  resulted in  
 445 a shielding shift of 0.7 ppm for TPSS( $\tau_0$ ).

446 The last row of the table shows the performance of the  
 447 KS(CCSD(T)) functional. This is in fact the current-independent  
 448 shielding  $\sigma_{\text{KS}}$  computed using the CCSD(T) density. This func-  
 449 tional is a close approximation to the shielding that would be  
 450 obtained from an exact, but current independent, DFT shield-  
 451 ing calculation. One sees that the error is surprisingly slightly  
 452 larger than the error of the KT2 functional. The reason that KT2  
 453 stands out from all other DFAs is that it has been directly fitted  
 454 to experimental shielding data. It is evident from the diamag-  
 455 netic performance and density error of KT2 that this fitting pro-  
 456 cedure has led to improved total shielding constants, but has  
 457 introduced other sources of errors in the functional. An improved  
 458 functional, KT3,<sup>15</sup> which remedies some of these errors, was later  
 459 introduced. However, KT3 does not give improved shielding con-  
 460 stants, and the authors remark that it gives rather poor electronic  
 461 energies. Since these energies contain the same expectation value  
 462  $\langle r^{-1} \rangle$  as the diamagnetic shielding constants it is likely that KT3  
 463 suffers from the same diamagnetic errors as KT2.

#### 464 4.4 Importance of current contributions to the exchange- 465 correlation energy

466 The method rankings in the last subsection, including the ranking  
 467 of the MP2 method, are very similar to those obtained for car-  
 468 bon and hydrogen by Flaig *et al.*<sup>2</sup> The DFA benchmark we have  
 469 just discussed is however flawed for our purpose, because current  
 470 independent DFAs are compared to reference numbers which in-  
 471 clude current effects. If a current correction is developed it should  
 472 be applied to a base functional that gets as close as possible to  
 473 the *current independent* shielding  $\sigma_{\text{KS}} = \sigma_{\text{dia}} + \sigma_{\text{para}}^{\text{para}}$ . Therefore  
 474 we have re-evaluated the performance of the DFAs benchmarked  
 475 in the previous section against the  $\sigma_{\text{KS}}$  numbers computed us-  
 476 ing CCSD(T) electron densities. The results are found in the two

477 rightmost columns of Table 2. The most striking feature of these  
 478 columns is that the performance of all DFAs, but one, improve sig-  
 479 nificantly. The standard deviations decrease by about 2 ppm, and  
 480 the average error decreases in magnitude by about 3-4 ppm. The  
 481 exception is KT2, which has a nearly unchanged average error but  
 482 an increase in the standard deviation by about 1 ppm.

483 Using the current independent reference values the ranking of  
 484 the DFAs changes. The best functional is now TPSS( $\tau_0$ ), followed  
 485 by cTPSS, while the best GGA functional is PBE. It is noteworthy  
 486 that, again, the gauge-dependent TPSS( $\tau_0$ ) performs better than  
 487 cTPSS. The reasons for that need to be explored in future work.  
 488 KT2 is now the second best functional overall, but in contrast to  
 489 the other functionals the current correction actually worsens its  
 490 performance.

491 The cTPSS functional is clearly an interesting case since it  
 492 already includes a current correction and so direct comparison  
 493 with the current independent benchmark values is not appropri-  
 494 ate. The current correction in cTPSS( $\tau_D$ ), arises naturally in the  
 495 Taylor expansion of the spherically averaged exchange hole as  
 496 shown by Dobson.<sup>39</sup> Unfortunately, since the current dependence  
 497 in cTPSS cannot be easily disentangled from the requirement for  
 498 gauge-invariance of  $E_{\text{xc}}$ , it is not easy to quantify the extent to  
 499 which the treatment of current effects is complete, nor how these  
 500 corrections interact with errors already present in the underly-  
 501 ing exchange-correlation functional form. Further investigation  
 502 of these points, including the worse performance of cTPSS com-  
 503 pared to TPSS, is left to further work. Nonetheless, it is notewor-  
 504 thy that cTPSS performs better than all DFAs except KT2 when  
 505 compared with CCSD(T) data. The quality of the current cor-  
 506 rected results can be compared to MP2, although it tends to un-  
 507 derestimate shielding constants by a similar extent to which MP2  
 508 overestimates.

## 509 5 Conclusions

510 By directly calculating the exchange correlation current contribu-  
 511 tion to NMR shielding constants (using CCSD(T), together with  
 512 the Wu-Yang method of obtaining the corresponding Kohn-Sham

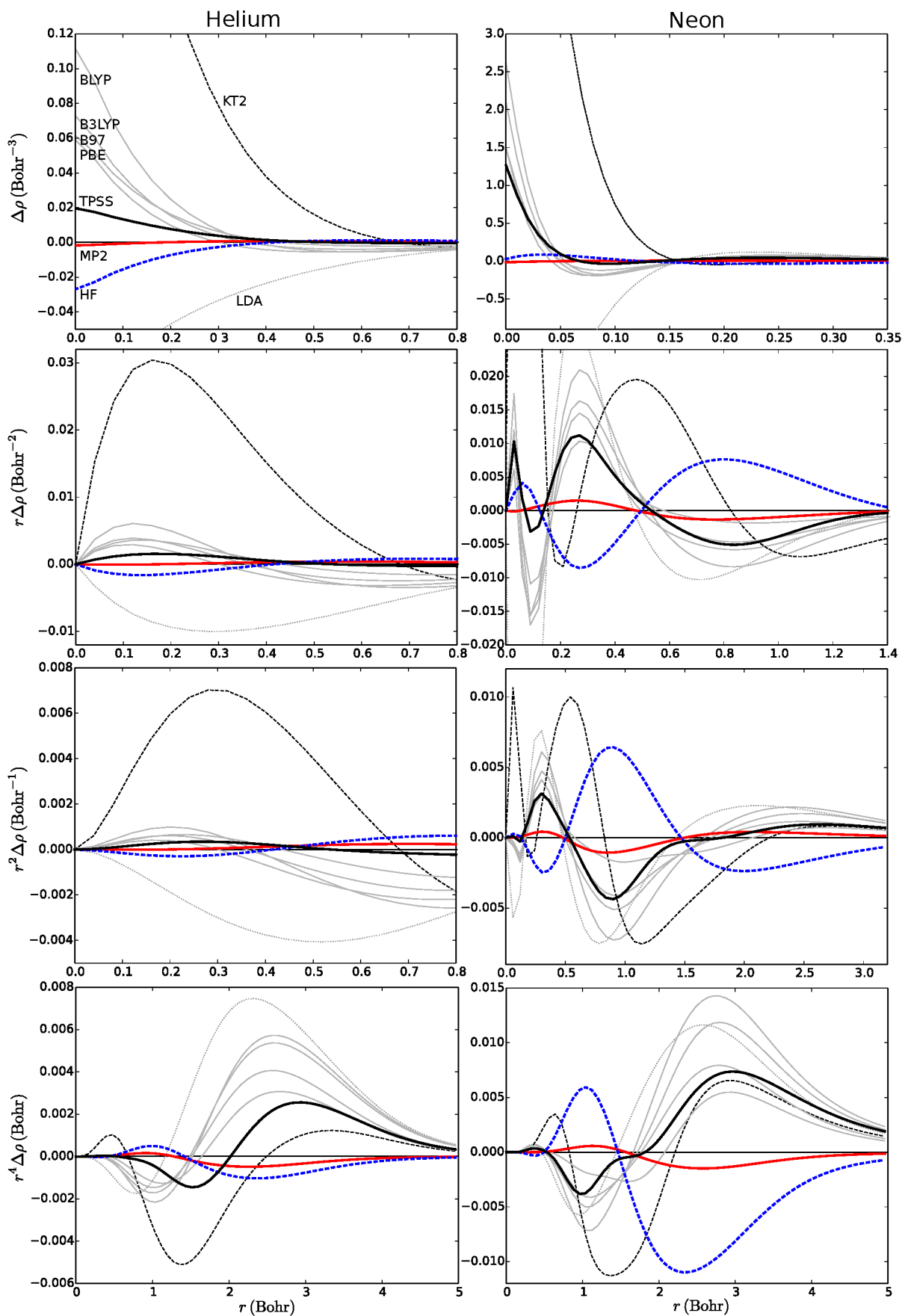


**Fig. 2** The density error  $\Delta\rho = \rho - \rho_{\text{CCSD(T)}}$  with weightings (from top to bottom) 1,  $r$ ,  $r^2$  and  $r^4$ , for the helium (left) and neon (right) atoms. The integral of the plotted functions corresponds to errors in the expectation value of  $\langle 1/r^2 \rangle$ ,  $\langle 1/r \rangle$ ,  $\langle 1 \rangle$  (particle number) and  $\langle r^2 \rangle$ , respectively. LDA is drawn using a thin dotted gray line, BLYP, B3LYP, PBE and B97 using solid thin gray line, KT2 thin dashed black line, TPSS black, HF dashed blue, MP2 red. The gray lines (GGA and hybrid functionals) are not intended to be distinguishable in this figure. Note the different scales in each subplot.

513 system) we have shown that the current contribution can in some  
514 cases amount to more than 10 ppm for carbon and nitrogen  
515 atoms. This means that the missing current contribution may be  
516 one of the leading causes of errors in shielding calculations using  
517 approximate DFT functionals. This also suggests that current in-  
518 dependent functionals should be judged based on their ability to  
519 reproduce accurate *ab initio* numbers with the current contribu-  
520 tion subtracted. As shown in Section 4.4 this reduces the average  
521 errors in the functionals, and in particular (c)TPSS, by several  
522 ppm. The exception is the empirical KT2 functional, which was  
523 fitted to experimental shielding data. As such the functional al-  
524 ready implicitly includes an empirical current correction, and it  
525 fits better to the current including benchmark set than the cur-  
526 rent free one.

527 In order to understand the large errors made by KT2 in the  
528 diamagnetic part of the shielding constant we have studied the  
529 ground state electron density for helium, neon, CO and N<sub>2</sub>. The  
530 origin of the errors in KT2 diamagnetic shieldings is clearly seen  
531 in the density, which has a very large error within 0.2 Bohr of the  
532 nucleus. The standard GGA functionals, and PBE in particular,  
533 give excellent diamagnetic shieldings, but still have large density  
534 error oscillations near the nucleus. Here TPSS stands out as the  
535 exchange-correlation functional with the most balanced density  
536 error. The MP2 methods gives densities with much smaller max-  
537 imum error than any density functional approximation, but for  
538 our test set of molecules this high accuracy is not needed for the  
539 purpose of NMR shieldings.

540 Since the current corrections ( $\sigma_j^{\text{para}}$  in Table 1) are comparable  
541 in magnitude to typical errors in approximate DFT shieldings ( $\Delta\sigma$   
542 in Table 2) it is important to develop good approximations to the  
543 current corrections. In this work we compute the correction us-  
544 ing CCSD(T), which is only useful for benchmark purposes. The  
545 data in the two rightmost columns of Table 2 indicate how differ-  
546 ent approximate functionals would perform with this correction  
547 added. In particular the cTPSS functional appears as a promising  
548 starting point for further development in this direction.

## 549 Acknowledgments

550 This work was supported by the Norwegian Research Coun-  
551 cil through the CoE Centre for Theoretical and Computational  
552 Chemistry (CTCC) Grant Nos. 179568/V30 and 171185/V30  
553 and through the European Research Council under the European  
554 Union Seventh Framework Program through the Advanced Grant  
555 ABACUS, ERC Grant Agreement No. 267683. A.M.T. is also grate-  
556 ful for support from the Royal Society University Research Fellow-  
557 ship scheme.

## References

- 558  
559 1 A. M. Teale, O. B. Lutnæs, T. Helgaker, D. J. Tozer and  
560 J. Gauss, *J. Chem. Phys.*, 2013, **138**, 024111.
- 561 2 D. Flaig, M. Maurer, M. Hanni, K. Braunger, L. Kick,  
562 M. Thubauville and O. C., *J. Chem. Theory Comput.*, 2014,  
563 **10**, 572–578.
- 564 3 G. Vignale and M. Rasolt, *Phys. Rev. Lett.*, 1987, **59**, 2360–  
565 2363.
- 566 4 C. J. Grayce and R. A. Harris, *Phys. Rev. A*, 1994, **50**, 3089–  
567 3095.
- 568 5 E. I. Tellgren, S. Kvaal, E. Sagvolden, U. Ekström, A. M. Teale  
569 and T. Helgaker, *Phys. Rev. A*, 2012, **86**, 062506.
- 570 6 A. M. Lee, N. C. Handy and S. M. Colwell, *J. Chem. Phys.*,  
571 1995, **103**, 10095–10109.
- 572 7 W. Zhu and S. B. Trickey, *J. Chem. Phys.*, 2006, **125**, 094317.
- 573 8 E. I. Tellgren, A. M. Teale, J. W. Furness, K. K. Lange, U. Ek-  
574 ström and T. Helgaker, *J. Chem. Phys.*, 2014, **140**, 034101.
- 575 9 W. Zhu, L. Zhang and S. B. Trickey, *Phys. Rev. A*, 2014, **90**,  
576 022504.
- 577 10 G. Schreckenbach and T. Ziegler, *J. Phys. Chem.*, 1995, **99**,  
578 606–611.
- 579 11 V. G. Malkin, O. L. Malkina, M. E. Casida and D. R. Salahub,  
580 *J. Am. Chem. Soc.*, 1994, **116**, 5898–5908.
- 581 12 P. J. Wilson, R. D. Amos and N. C. Handy, *Mol. Phys.*, 1999,  
582 **97**, 757–768.
- 583 13 P. J. Wilson and D. J. Tozer, *Chem. Phys. Lett.*, 2001, **337**,  
584 341–348.
- 585 14 T. W. Keal and D. J. Tozer, *J. Chem. Phys.*, 2003, **119**, 3015–  
586 3024.
- 587 15 T. W. Keal and D. J. Tozer, *J. Chem. Phys.*, 2004, **121**, 5654.
- 588 16 S. J. Vosko, L. Wilk and M. Nusair, *Can. J. Phys.*, 1980, **58**,  
589 1200.
- 590 17 C. Lee, W. Yang and R. G. Parr, *Phys. Rev. B*, 1988, **37**, 785–  
591 789.
- 592 18 A. D. Becke, *J. Chem. Phys.*, 1988, **88**, 1053–1062.
- 593 19 J. P. Perdew, K. Burke and M. Ernzerhof, *Phys. Rev. Lett.*, 1996,  
594 **77**, 3865–3868.
- 595 20 A. D. Becke, *J. Chem. Phys.*, 1997, **107**, 8554–8560.
- 596 21 A. D. Becke, *J. Chem. Phys.*, 1993, **98**, 1372–1377.
- 597 22 J. Tao, J. P. Perdew, V. N. Staroverov and G. E. Scuseria, *Phys.*  
598 *Rev. Lett.*, 2003, **91**, 146401.
- 599 23 J. Gauss and J. F. Stanton, *J. Chem. Phys.*, 1996, **104**, 2574.
- 600 24 T. Helgaker, M. Jaszuński and K. Ruud, *Chem. Rev.*, 1999, **99**,  
601 293–352.
- 602 25 F. London, *J. Phys. Radium*, 1937, **8**, 397–409.
- 603 26 T. Helgaker, P. J. Wilson, R. D. Amos and N. C. Handy, *J.*  
604 *Chem. Phys.*, 2000, **113**, 2983–2989.
- 605 27 S. Kvaal, U. Ekström, A. M. Teale and T. Helgaker, *J. Chem.*  
606 *Phys.*, 2014, **140**, 18A518.
- 607 28 S. M. Colwell and N. C. Handy, *Chem. Phys. Lett.*, 1994, **217**,  
608 271 – 278.
- 609 29 Q. Zhao, R. Morrison and R. Parr, *Phys. Rev. A*, 1994, **50**, 2138.
- 610 30 Q. Wu and W. T. Yang, *J. Chem. Phys.*, 2003, **118**, 2498–2509.
- 611 31 A. M. Teale, S. Coriani and T. Helgaker, *J. Chem. Phys.*, 2010,  
612 **132**, 164115.
- 613 32 CFOUR, a quantum chemical program package written by J.F.  
614 Stanton, J. Gauss, M.E. Harding, P.G. Szalay with contribu-  
615 tions from A.A. Auer, R.J. Bartlett, U. Benedikt, C. Berger, D.E.  
616 Bernholdt, Y.J. Bomble, L. Cheng, O. Christiansen, M. Heck-  
617 ert, O. Heun, C. Huber, T.-C. Jagau, D. Jonsson, J. Jusélius, K.  
618 Klein, W.J. Lauderdale, D.A. Matthews, T. Metzroth, L.A. Mück,  
619 D.P. O'Neill, D.R. Price, E. Prochnow, C. Puzzarini, K. Ruud,  
620 F. Schiffmann, W. Schwalbach, C. Simmons, S. Stopkowitz, A.  
621 Tajti, J. Vázquez, F. Wang, J.D. Watts and the integral pack-  
622 ages MOLECULE (J. Almlöf and P.R. Taylor), PROPS (P.R. Tay-  
623 lor), ABACUS (T. Helgaker, H.J. Aa. Jensen, P. Jørgensen, and  
624 J. Olsen), and ECP routines by A. V. Mitin and C. van Wüllen.  
625 For the current version, see <http://www.cfour.de>.
- 626 33 Dalton, a molecular electronic structure program, Release Dal-  
627 ton2015.0 (2015), see <http://daltonprogram.org>.
- 628 34 K. Aidas, C. Angeli, K. L. Bak, V. Bakken, R. Bast, L. Boman,  
629 O. Christiansen, R. Cimiraglia, S. Coriani, P. Dahle, E. K. Dal-  
630 skov, U. Ekström, T. Enevoldsen, J. J. Eriksen, P. Ettenhu-  
631 ber, B. Fernández, L. Ferrighi, H. Fliegl, L. Frediani, K. Hald,  
632 A. Halkier, C. Hättig, H. Heiberg, T. Helgaker, A. C. Hen-  
633 num, H. Hettema, E. Hjertenæs, S. Høst, I.-M. Høyvik, M. F.  
634 Iozzi, B. Jansík, H. J. Aa. Jensen, D. Jonsson, P. Jørgensen,  
635 J. Kauczor, S. Kirpekar, T. Kjærgaard, W. Klopper, S. Knecht,  
636 R. Kobayashi, H. Koch, J. Kongsted, A. Krapp, K. Kristensen,  
637 A. Ligabue, O. B. Lutnæs, J. I. Melo, K. V. Mikkelsen, R. H.  
638 Myhre, C. Neiss, C. B. Nielsen, P. Norman, J. Olsen, J. M. H.  
639 Olsen, A. Osted, M. J. Packer, F. Pawłowski, T. B. Pedersen,  
640 P. F. Provasi, S. Reine, Z. Rinkevicius, T. A. Ruden, K. Ruud,  
641 V. V. Rybkin, P. Sałek, C. C. M. Samson, A. S. de Merás,  
642 T. Saue, S. P. A. Sauer, B. Schimmelpfennig, K. Sneskov,  
643 A. H. Steindal, K. O. Sylvester-Hvid, P. R. Taylor, A. M. Teale,  
644 E. I. Tellgren, D. P. Tew, A. J. Thorvaldsen, L. Thøgersen,  
645 O. Vahtras, M. A. Watson, D. J. D. Wilson, M. Ziolkowski and  
646 H. Ågren, *WIREs Comput. Mol. Sci.*, 2015, **4**, 269–284.
- 647 35 LONDON, an ab-initio program package for calculations in fi-  
648 nite magnetic fields, founded by E. I. Tellgren, A. Soncini and T.  
649 Helgaker. Programming by E. I. Tellgren (main programmer),  
650 K. K. Lange, A. M. Teale, U. E. Ekström, S. Stopkowitz and J. H.  
651 Austad.
- 652 36 E. I. Tellgren, A. Soncini and T. Helgaker, *J. Chem. Phys.*,  
653 2008, **129**, 154114.
- 654 37 S. N. Maximoff and G. E. Scuseria, *Chem. Phys. Lett.*, 2004,  
655 **390**, 408–412.
- 656 38 E. Sagvolden, U. Ekström and E. Tellgren, *Mol. Phys.*, 2013,  
657 **111**, 1295–1302.
- 658 39 J. F. Dobson, *J. Chem. Phys.*, 1993, **98**, 8870.
- 659 40 A. D. Becke, *J. Chem. Phys.*, 2002, **117**, 6935.
- 660 41 J. Tao, *Phys. Rev. B*, 2005, **71**, 205107.
- 661 42 J. E. Bates and F. Furche, *J. Chem. Phys.*, 2012, **137**, 164105.
- 662 43 J. W. Furness, J. Verbeke, E. I. Tellgren, S. Stopkowitz,  
663 U. Ekström, T. Helgaker and A. M. Teale, *In preparation*  
664 ([arXiv:1505.07989 \[physics.chem-ph\]](https://arxiv.org/abs/1505.07989)), 2015.
- 665 44 J. Gauss, K. Ruud and T. Helgaker, *J. Chem. Phys.*, 1996, **105**,

- 666 2804–2812.
- 667 45 T. H. Dunning, *J. Chem. Phys.*, 1989, **90**, 1007–1023.
- 668 46 D. E. Woon and T. H. Dunning, *J. Chem. Phys.*, 1994, **100**,  
669 2975–2988.
- 670 47 T. Helgaker and P. Jørgensen, *J. Chem. Phys.*, 1991, **95**, 2595–  
671 2601.
- 672 48 K. Jankowski, K. Nowakowski, I. Grabowski and  
673 J. Wasilewski, *J. Chem. Phys.*, 2009, **130**, 164102.
- 674 49 I. Grabowski, A. M. Teale, S. Śmiga and R. J. Bartlett, *J. Chem.*  
675 *Phys.*, 2011, **135**, 114111.